RESEARCH ARTICLE

morphology WILEY

Distal leg structures of the Aculeata (Hymenoptera): A comparative evolutionary study of *Sceliphron* (Sphecidae) and *Formica* (Formicidae)

Rolf Georg Beutel[1] | Adrian Richter[1] | Roberto A. Keller[2] |
Francisco Hita Garcia[3] | Yoko Matsumura[4] | Evan P. Economo[3] | Stanislav N. Gorb[4]

[1]Institut für Zoologie und Evolutionsforschung, Friedrich-Schiller-Universität, Jena, Germany

[2]Museu Nacional de Historia Natural e da Ciência and Centre for Ecology, Evolution and Environmental Changes, Universidade de Lisboa, Lisbon, Portugal

[3]Biodiversity and Biocomplexity Unit, Okinawa Institute of Science and Technology Graduate University, Okinawa, Japan

[4]Department of Functional Morphology and Biomechanics, Zoological Institute, Kiel University, Kiel, Germany

Correspondence
Adrian Richter, Institut für Zoologie und Evolutionsforschung, Friedrich-Schiller-Universität, Erbertstr. 1, Jena 07743, Germany.
Email: adrian.richter@uni-jena.de

Abstract

The distal parts of the legs of *Sceliphron caementarium* (Sphecidae) and *Formica rufa* (Formicidae) are documented and discussed with respect to phylogenetic and functional aspects. The prolegs of Hymenoptera offer an array of evolutionary novelties, mainly linked with two functional syndromes, walking efficiently on different substrates and cleaning the body surface. The protibial-probasitarsomeral cleaning device is almost always well-developed. A complex evolutionary innovation is a triple set of tarsal and pretarsal attachment devices, including tarsal plantulae, probasitarsomeral spatulate setae, and an arolium with an internal spring-like arcus, a dorsal manubrium, and a ventral planta. The probasitarsal adhesive sole and a complex arolium are almost always preserved, whereas the plantulae are often missing. *Sceliphron* has retained most hymenopteran ground plan features of the legs, and also *Formica*, even though the adhesive apparatus of Formicidae shows some modifications, likely linked to ground-oriented habits of most ants. Plantulae are always absent in extant ants, and the arolium is often reduced in size, and sometimes vestigial. The arolium contains resilin in both examined species. Additionally, resilin enriched regions are also present in the antenna cleaners of both species, although they differ in which of the involved structures is more flexible, the calcar in *Sceliphron* and the basitarsal comb in *Formica*. Functionally, the hymenopteran distal leg combines (a) interlocking mechanisms (claws, spine-like setae) and (b) adhesion mechanisms (plantulae, arolium). On rough substrate, claws and spine-like setae interlock with asperities and secure a firm grip, whereas the unfolding arolium generates adhesive contact on smooth surfaces. Differences of the folded arolium of *Sceliphron* and *Formica* probably correlate with differences in the mechanism of folding/unfolding.

KEYWORDS
adhesion, antenna cleaner, arolium, proleg, tarsus

1 | INTRODUCTION

Among well-known synapomorphies of Hymenoptera like the wing coupling mechanism with hamuli or the haploid-diploid reproductive system (e.g., Beutel et al., 2014; Rasnitsyn, 1988), the prolegs offer an array of evolutionary novelties supporting the group as a clade. This character complex is mainly linked to two functional syndromes, walking efficiently on different substrates, especially plant surfaces (e.g., Beutel & Gorb, 2001), and cleaning the body surface, which is usually characterized by an exceptionally rich vestiture of different hairs and sensilla.

As shown previously (e.g., Basibuyuk & Quicke, 1995; Frantsevich & Gorb, 2002; Frantsevich & Gorb, 2004; Gladun, 2008; Gladun, Gorb, & Frantsevich, 2009; Snodgrass, 1956), structural features of the distal leg of Hymenoptera are exceptionally complex and arguably a key character system in the evolution of the megadiverse order. Distal leg structures of insects, especially adhesive devices, have attracted considerable attention from researchers over the years (see Beutel & Gorb, 2001, 2006 for an overview). These critical components of the phenotype are linked to the abilities of organisms to move, land, grab, manipulate, and interact with other organisms, especially plants. An early comparative study of insect attachment structures was presented by De Meijere (1901), and a consistent terminology was introduced by Dashman (1953). Functional aspects were investigated in numerous studies, such as, for instance, Drechsler and Federle (2006), Bullock, Drechsler, and Federle (2008), or Endlein and Federle (2015) (see also Gorb (2010) for an overview). The first comprehensive evaluation of the character evolution was presented by Beutel & Gorb (2001) (see also Beutel & Gorb, 2006, 2008). Gorb and Beutel (2001) pointed out that adhesive devices of pterygote insects and surfaces of plants experienced a remarkable coevolutionary history, which resulted in the exceptionally high diversity of angiosperm plants, and in an unparalleled diversification in insects, especially in the "BIG4" of Holometabola, Diptera, Lepidoptera, Coleoptera, and Hymenoptera (e.g., Lambkin et al., 2013; McKenna et al., 2019; Misof et al., 2014; Peters et al., 2017; Rasnitsyn, 1988; Regier et al., 2013; Ronquist et al., 2012; Ronquist, Rasnitsyn, Roy, Eriksson, & Lindgren, 1999; Sharkey et al., 2012).

Attachment devices of the megadiverse Hymenoptera have also been studied intensively. Snodgrass (1956), in his magisterial work on the anatomy of the honeybee, described and illustrated the adhesive devices of *Apis mellifera* Linnaeus in detail. Frantsevich and Gorb (2002, 2004) described pretarsal and tarsal elements of species of Vespidae and analyzed functional aspects of different parts of the system. Schulmeister (2003) addressed the evolution of plantulae in Hymenoptera, with emphasis on the basal lineages. The complex pretarsal structures were treated by Gladun (2008), Gladun and Gumovsky (2006) and Gladun et al. (2009). Characters of the distal leg were also covered in a broad treatment of the hymenopteran mesosoma by Vilhelmsen, Miko, and Krogmann (2010).

The adhesive devices and the attachment performance of ants were also intensively studied (e.g., Brainerd, 1994; Endlein & Federle, 2015; Federle, Maschwitz, Fiala, Riederer, & Hölldobler, 1997; Federle, Rohrseitz, & Hölldobler, 2000; Hölldobler & Palmer, 1989; Orivel, Malherbe, & Dejean, 2001). For example, Orivel et al. (2001) compared the performance of various ponerine genera in the context of an arboreal lifestyle. However, these contributions have primarily focused on function rather than morphology, and comparative aspects have played only a minor role in studies on ant legs and specifically attachment structures. This leaves many questions about how leg structures evolved along with the diversification of ants into ecological and behavioral niche space.

Compared to attachment structures, cleaning organs have received relatively little attention. The grooming behavior of Zoraptera and Embioptera was described by Valentine (1986). The protibial antenna cleaner of ground beetles has been recognized as phylogenetically important character system (e.g., Beutel, 1992), and also the lepidopteran protibial epiphysis (or spur; e.g., Kristensen & Skalski, 1999). Otherwise, studies on grooming devices were largely restricted to Hymenoptera. The morphology of the antenna cleaner, especially of non-aculeatan families, was treated in Basibuyuk and Quicke (1995), and the phylogenetic significance of the grooming behavior in Hymenoptera by Basibuyuk and Quicke (1999). Comparative studies on the strigil of ants were presented by Francoeur and Loiselle (1988) and Keller (2011), and the efficacy of the antenna cleaner of *Camponotus rufifemur* Emery was evaluated by Hackmann, Delacave, Robinson, Labonte, and Federle (2015). A phylogenetic study of the antenna cleaner in Formicidae, Mutillidae, and Tiphiidae was presented by Schönitzer and Lawitzky (1987), and the antenna cleaner of *Messor rufitarsus* (Fabricius) was described in detail by Schönitzer, Dott, and Melzer (1996).

The purpose of the present study is to describe and document the distal parts of the legs including cleaning and adhesive devices of *Formica rufa* Linnaeus, a generalist species of Formicinae, and of the wasp *Sceliphron caementarium* (Drury) of Sphecidae (as defined in Sann et al. (2018)), a group nested within Apoidea, which is the sister taxon to the ants (Branstetter, Danforth, et al., 2017; Branstetter, Longino, et al., 2017; Johnson et al., 2013; Peters et al., 2017). The main emphasis is on the complex distal part of the forelegs. The observed characters are compared with data in the literature (e.g., Basibuyuk & Quicke, 1995; Frantsevich & Gorb, 2002; Gladun, 2006; Keller, 2011; Schulmeister, 2003; Vilhelmsen et al., 2010) and evaluated with respect to their functional and phylogenetic background. We discuss evolutionary transformations of this complex character system in Hymenoptera with special emphasis on the ground plan of Hymenoptera and Formicidae. While focusing on just two species, this study aims to establish a framework of homologies to map the full diversity of leg structures in ants, to compare them with homologous elements in other groups of Hymenoptera, and to trace the evolution of the character system.

2 | MATERIAL AND METHODS

2.1 | List of taxa examined

Xyelidae: *Macroxyela ferruginea* (Say), *Xyela julii* (Brébisson).
Pamphiliidae: *Onycholyda luteicornis* (Norton).
Siricidae: *Urocerus gigas* Linnaeus.

Sphecidae: *S. caementarium* (Drury).

Apidae: *A. mellifera* Linnaeus.

Vespidae: *Paravespula germanica* (Fabricius).

Formicidae, Formicinae: *F. rufa* Linnaeus, *Cataglyphis* Foerster sp.

Dorylinae: *Dorylus* Fabricius sp. (males).

Ponerinae: *Diacamma* Mayer sp.

Myrmicinae: *Messor* Forel sp.

2.2 | Scanning electron microscopy

Samples in 70% ethanol were dehydrated in a rising ethanol series (80, 90, 96, and 100%), transferred to 100% acetone, and subsequently dried at the critical point in liquid CO_2 using an Emitech K 850 Critical Point Dryer (Sample Preparation Division, Quorum Technologies Ltd., Ashford, England). Dried Samples were glued to minute needles with super glue and mounted on a rotatable specimen holder (Pohl 2010). An Emitech K 500 (Sample Preparation Division, Quorum Technologies Ltd.) was used for sputter coating with gold. Scanning electron microscopy (SEM) micrographs were taken with a Philips ESEM XL30 (Philips, Amsterdam, Netherlands) equipped with Scandium FIVE software (Olympus, Münster, Germany).

2.3 | Confocal laser scanning microscopy

To visualize autofluorescences of adhesion pads and antenna cleaners, we applied a method established by Michels and Gorb (2012) using a confocal laser scanning microscope Zeiss LSM 700 (Carl Zeiss Microscopy GmbH, Jena, Germany). Following Michels and Gorb (2012), we visualized autofluorescences of the adhesion pads and antenna cleaners using four different stable solid lasers with wavelengths of 405, 488, 555, and 639 nm as excitation wavelengths and a band-pass emission filter, transmitting light with wavelengths 420–480 nm, and long-pass emission filters to detect selective emitted autofluorescences, respectively.

The confocal laser scanning microscopy (CLSM) based method was originally described based on specimens being freshly frozen and stored at −70°C (Michels & Gorb, 2012). However, for this study, mainly specimens preserved in 70% ethanol were available. Therefore, we tested if images would differ between specimens preserved freshly or in 70% ethanol using *Messor* sp. All 70% ethanol preserved specimens were submerged in distilled water at least for one night to hydrate specimens before the CLSM analyses. Then, they were transferred to and rinsed in glycerin (≥99.5%, free of water, Carl Roth GmbH & Co., KG, Karlsruhe, Germany) and then mounted in glycerin droplets on glass slides. Depending on the size of specimens, we used either an objective lens ×10 (Zeiss Plan-Apochromat, numerical aperture: 0.45) or ×20 (Zeiss Plan-Apochromat, numerical aperture: 0.8). All images were taken separately, and we optimized CLSM settings for each specimen. Following Michels and Gorb (2012), we interpreted the results as follows: red-colored areas are relatively stiff, green-colored ones are tough and flexible, and blue-colored ones are resilin enriched.

2.4 | Microtome section series

Distal parts of legs (tarsus and pretarsus) were removed with Dumont forceps. Dehydration of the samples was performed as described for drying at the critical point, followed by embedding in Araldite CY 212 (Agar Scientific, Stansted/Essex, England). The samples were sectioned (0.5 μm thickness) with a microtome HM 360 (Microm, Walldorf, Germany) equipped with a diamond knife. The sections were stained with toluidine blue and pyronine G (Waldeck GmbH & Co. KG/Chroma Division, Münster, Germany) and examined with an Axioscope (Carl Zeiss AG, Oberkochen, Germany).

2.5 | Microtomography, 3D reconstruction, and material segmentation

A fore leg of *Sceliphron* previously prepared for SEM imaging was inserted into a fine pipette tip which was attached to a microtomography (μCT)-sample holder. The sample was μCT-scanned using a Bruker Skyscan 2211 μCT scanner (Bruker, Belgium) at the Max-Planck-Institut für Menschheitsgeschichte Jena, Germany, equipped with a high-resolution (4,000 × 2,600 pixel) X-ray sensitive CCD camera. A beam strength of 40 kV and 120 μA was employed. Exposure time was 850 ms and an image pixel size of 1.77 μm was chosen in a 360° scan with 0.2° rotation steps. Tomographic reconstruction was done using NRecon (Version: 1.7.3.1). The fore leg of *F. rufa* was similarly inserted into a very fine pipette tip and then attached to a μCT sample holder. The μCT scanner used was a Zeiss Xradia 510 Versa 3D X-ray microscope operated with the Zeiss Scout-and-Scan Control System software (version 11.1.6411.17883) at the Okinawa Institute of Science and Technology Graduate University, Japan. The scanning parameters chosen consisted of a 40 kV (75 μA)/3 W beam strength with 6 s exposure time under a × 4 magnification, which resulted in a voxel size of 1.81 μm. 3D reconstructions of the resulting scan projection data were done with the Zeiss Scout-and-Scan Control System Reconstructor (version 11.1.6411.17883) and saved in DICOM file format. Post-processing of DICOM raw data was done with Amira 6.0 software (Visage Imaging GmbH, Berlin, Germany) in order to segment individual structures into discrete materials. The segmented materials were then exported with the plugin script "multiExport" (Engelkes, Friedrich, Hammel, & Haas, 2018) in Amira 6.1 as Tiff image stacks. VG-Studio Max 2.0 (Volume Graphics GmbH, Heidelberg, Germany) was used to create volume renders out of the Tiff image series.

2.6 | Image processing

All images were edited using Adobe Photoshop CS6 (Adobe Systems Incorporated, San Jose, CA) and arranged into figure plates. On SEM

images and images from section series, tonal correction was performed. The selective sharpener (30% strength) was used on all images. Adobe Illustrator CS6 (Adobe Systems Incorporated) was used to label the figure plates.

2.7 | Terminology

The terminology of the leg and its adhesive devices is based on Basibuyuk and Quicke (1995) and Beutel and Gorb (2001).

3 | RESULTS

3.1 | Hymenoptera

This section is based on observations made with the examined material, but also on earlier studies (e.g., Basibuyuk & Quicke, 1995; Beutel & Gorb, 2001, 2006; Rasnitsyn, 1988; Schulmeister, 2003; Snodgrass, 1956; Vilhelmsen et al., 2010).

The length of the legs increases from anterior to posterior in most groups. A dense vestiture of fine setae is almost always present. The
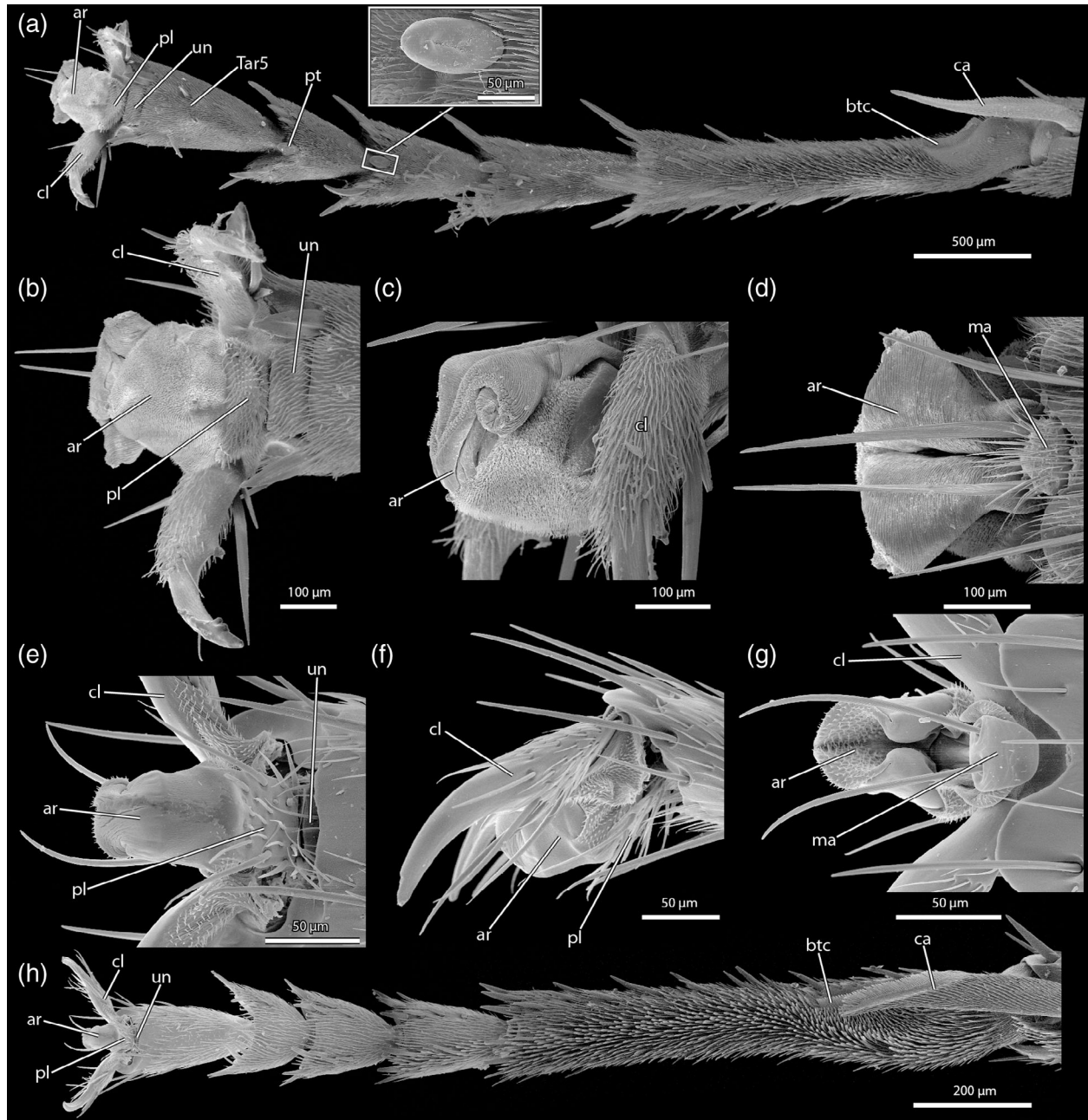
FIGURE 1 *S. caementarium* (Sphecidae) (a–d) and *F. rufa* (Formicidae) (e–h), scanning electron micrographs of the foreleg tarsi of females (worker caste in case of *Formica*). (a,h) Overview of protarsus in ventral view, insert in (a) shows tarsal plantula. (b,e) Ventral view of pretarsal structures. (c,f) Lateral view on pretarsal structures. (d,g) Dorsal view on pretarsal structures. ar, arolium; btc, basitarsal comb; ca, calcar; cl, claw; ma, manubrium; pl, planta; pt, plantula; Tar5, tarsomere 5; un, unguitractor plate

tarsus is usually composed of five tarsomeres. Four- or three-segmented tarsi occur only in few groups, probably linked with miniaturization (e.g., Chalcidoidea part., Platygasteridae, Trichogrammatidae; Naumann, 1991). The forelegs bear the elements of the antenna cleaning device. The protibial calcar is present in the ground plan of Hymenoptera, and the probasitarsal notch and comb in Orussidae and Aculeata (Vilhelmsen et al., 2010). Tarsal plantulae are usually present, either fixed or articulated (Beutel & Gorb, 2006; Schulmeister, 2003). The basitarsomere bears a dense sole of tenent setae (sensu Dashman (1953)), likely an autapomorphy of the order. The arolium is well developed in almost all groups. It is supported by the arcus, a spring-like element and unique among Hexapoda. The arolium is supported by the plate-like planta on the ventral side, which is adjacent with the unguitractor plate. A manubrium is present dorsally, apically inserted on tarsomere 5. The claws are often pubescent proximally and usually bear a mesal tooth and several setae.

## 3.2 | *Sceliphron* (Sphecidae)

The five-segmented (pentamerous) tarsi of the three legs are similar in their general organization, but differ distinctly in size, with a length ratio of 1:1.5:2 from anterior to posterior. The prolegs also differ by the presence of the antenna cleaning organ, with a specialized apical tibial spur and a shallow notch of the probasitarsomere (Figures 1a and 2a,b). The distal half of the metafemur is black; the other parts of the hind legs are mostly yellowish to light brown. The apical parts of the mesotarsomere and metatarsomere are almost black. The two distal tarsomeres of the middle and hind legs are also more strongly pigmented, and also the three distal protarsomeres. All three pairs of legs are pubescent, with the surface almost entirely covered with a dense, regularly arranged vestiture of fine, short setae, varying in length between about 0.02 and 0.03 mm and also slightly in thickness; the individual hairs are mostly oriented toward the apex of the leg.

Setae and spine-like strengthened setae of different length and different patterns of arrangement are present on different regions of the tarsomeres, especially concentrated on the apical portions, but largely missing on the dorsal surface. With about 1.7 mm, the probasitarsomere is by far the longest segment of the tarsus of the foreleg (Figure 1a). It is about 0.3 mm wide at its base. The basalmost portion following the articulation with the tibia is distinctly curved. A concavity of the proximoventral part of the probasitarsomere (Keller, 2011: probasitarsal notch) contains the basitarsal comb of the strigil (Basibuyuk & Quicke, 1995; btc, Figures 2a,b and 3c), about 0.3 mm long and formed by very densely and regularly arranged stiff microtrichia (ca. 0.05 mm), situated on relatively flexible cuticle (Figure 3c) close to the posterior margin of the tarsal segment. Some of the microtrichia show resilin (blue) signal on CLSM images
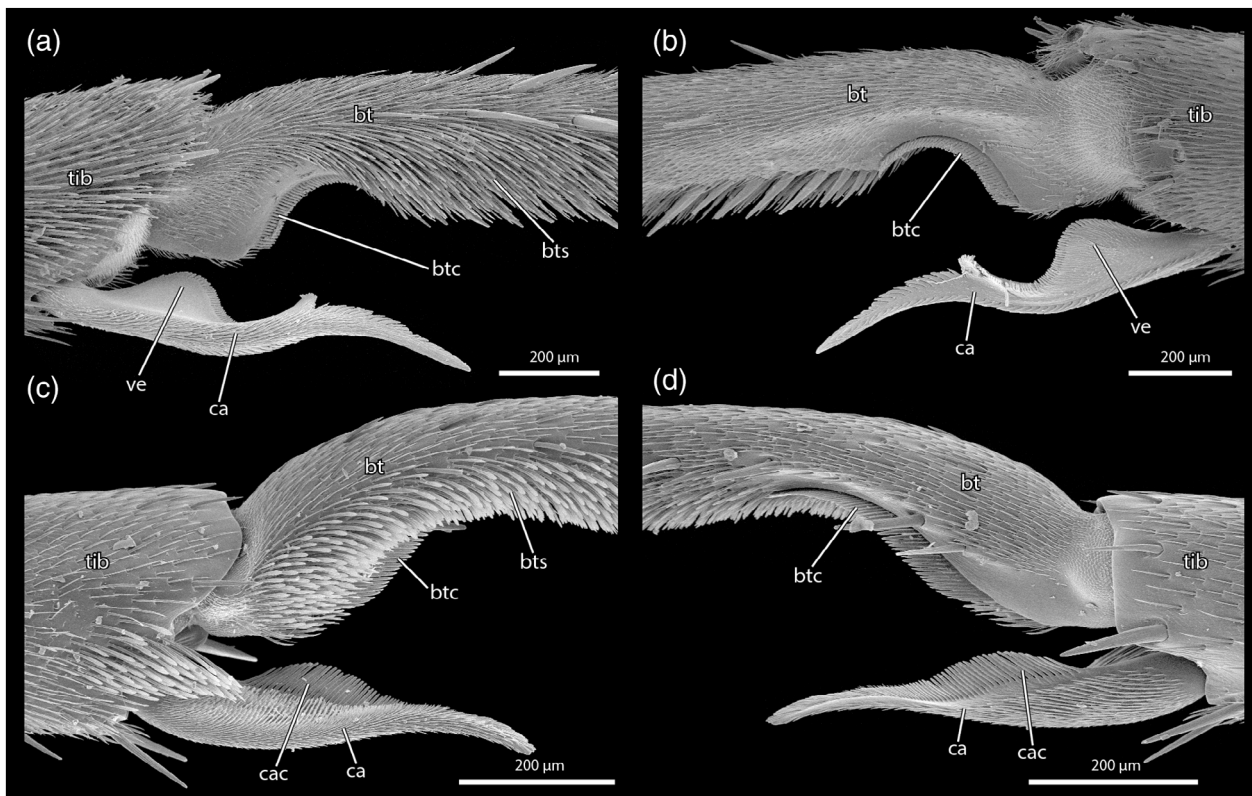
FIGURE 2 *S. caementarium* (Sphecidae) (a,b) and *F. rufa* (Formicidae) (c,d), scanning electron micrographs of the antenna cleaner on the forelegs of females (worker caste in case of *Formica*). (a,c) Antenna cleaner in anterior view. (b,d) Antenna cleaner in posterior view. bt, basitarsus; btc, basitarsal comb; bts, basitarsal spatulate setae; ca, calcar; cac, comb of the calcar; tib, tibia; ve, velum of the calcar
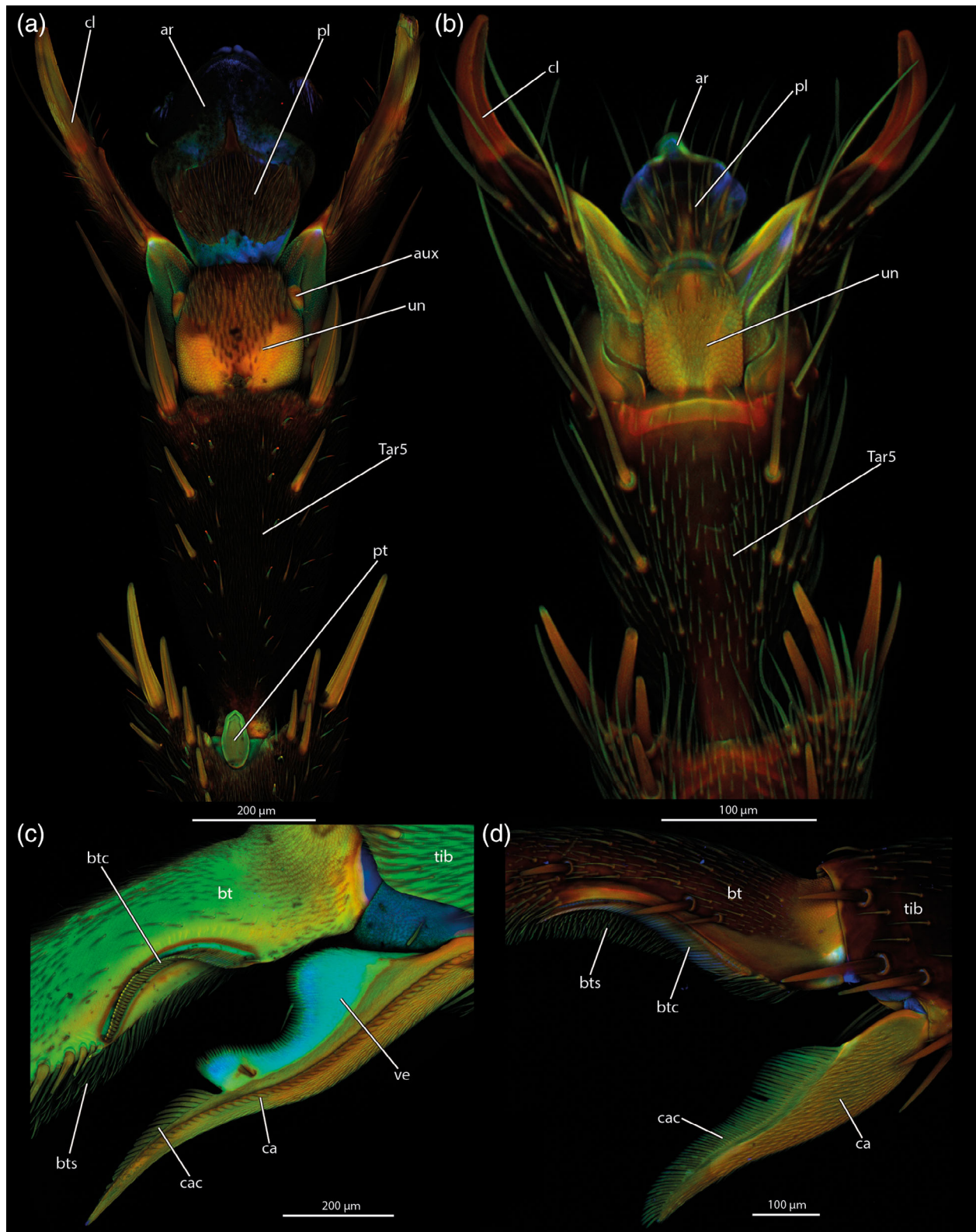
FIGURE 3 *S. caementarium* (Sphecidae) (a,c) and *F. rufa* (Formicidae) (b,d), confocal laser scanning microscopic images of tarsomere 5 of a female (worker in case of *Formica*) foreleg, both in ventral view (a,b) and confocal laser scanning microscopy (CLSM) images of the antenna cleaner in posterior view (c,d). ar, arolium; aux, auxiliary sclerites; bt, basitarsus; btc, basitarsal comb; bts, basitarsal spatulate setae; ca, calcar; cac, comb of the calcar; cl, claw; pl, planta; pt, plantula; Tar5, tarsomere 5; tib, tibia; un, unguitractor plate; ve, velum of the calcar

(Figure 3c). A sinuate field with a smooth surface is adjacent with the comb on the ventral side and reaches the articulation with the tibia proximally. The basitarsal comb is followed by a regular row of longer setae (ca. 0.1 mm) on the ventral surface, close to the posterior edge. It nearly reaches the apex of the tarsal segment. The posterior edge of the tarsomere bears similar setae, but less regularly arranged and more widely spaced. The entire ventral surface except for the area of the cleaning organ bears a dense hairy sole of thin tenent hairs (ca. 0.05 mm long) with a slightly extended, spatulate apex (Basibuyuk & Quicke, 1995: paddle-shaped setae; Figure 2a). Only few longer setae insert on the dorsal, anterior, and posterior surfaces. The apical portion of the probasitarsomere is truncated, without lateral lobes or extensions. It bears a dense array of spine-like setae, especially on the ventral side, three of them distinctly longer than the others (ca. 0.2–0.25 mm), flattened, blade-like, and strengthened by a low and narrow median longitudinal ridge. The longest one is posteriorly directed, the slightly shorter ones anteriorly. A distinct oval plantula with a very smooth surface, about 0.09 mm long, is inserted ventromedially.

The anterior tibial spur, the calcar of the strigil, inserts ventrally in a distinct notch of the apical tibial margin (ca. Figures 1a, 2a,b, and 3c). An unsclerotized, white pad-like structure with high resilin signal inserts at the base, with a dense vestiture of extremely short microtrichia (Figure 3c). The posterior tibial spur is missing. The calcar is about 0.8 mm long and slightly sinuate, tapering distally, with a single pointed apex. The entire structure bears an extremely dense vestiture of slightly curved and apically pointed microtrichia. An equally dense row of slightly longer and flattened tooth-like spines without basal articulations is present along the resilin-enriched ventral margin (Figure 3c). A thin and transparent triangular lamellum (velum, ve; Figure 2a,b) with high resilin content (Figure 3c) is present on the opposite edge, slightly longer than the concavity of tarsomere 1, and also equipped with a dense comb of stiff microtrichia.

Protarsomere 2 is less than half as long as the probasitarsomere. Its base is distinctly narrower than that of the proximal tarsomere, but it is widening distally (Figure 1a). Between the fine pubescence, some longer and thicker setae are inserted like on the surface of the probasitarsomere. A regular median row of spine-like setae (ca. 0.1 mm) is present on the ventral side, and an additional shorter row on the distal half of the posterior edge. Few longer setae are present on the anterior surface of the segment. The distal edge is slightly emarginated. The plantula and vestiture of apical spine-like setae are similar to those of tarsomere 1.

Protarsomere 3 is slightly shorter than 2. It is distinctly widening distally and the apical emargination is more distinct than that of tarsomere 2. Otherwise the shape and vestiture are similar, including the ventromedian row of spine-like setae, the plantula (Figure 1a, box), and the spine-like setae of the apical region.

Protarsomere 4 is again slightly shorter than the preceding segment. It is distinctly narrowed basally and strongly widening distally, thus appearing almost triangular. The apical emargination is deeper, resulting in a bilobed shape of the distal margin. The median longitudinal row of spine-like setae is missing. A plantula is present.

The apical protarsomere 5 is almost as long as 3 and 4 combined (ca. 0.7 mm). It is also strongly narrowed basally but distinctly widening distally, especially in the proximal 1/3. The ventral surface bears two longer and several short setae. The pubescence on the dorsal side of the tarsomere is regular, without interspersed longer hairs except for two pairs of long setae on the apical region, the inner ones about 0.25 mm and the outer ones about 0.3 mm long. The apical margin is oblique with a longer dorsal end (Figure 3d). The dorsal side is bilobed, with two rounded lateral lobes separated by a median emargination, which bears the manubrium. The manubrium appears as a small semicircular plate in dorsal view (ma, Figures 1d and 4b,e), about 0.1 mm wide, with the normal fine pubescence on its dorsal surface, and slightly longer hairs close to the apical margin. A pair of long setae (ca. 0.35 mm) with a longitudinally riffled surface is inserted distally on this plate. A tapering, slightly sinuous stalk of the plate reaches between the fold of the arolium, resulting in a club-shaped appearance of the manubrium (ma, Figures 4c,d and 5c).

The well-sclerotized unguitractor plate, an almost quadrangular sclerite with rounded lateral edges, inserts in an emargination of the ventral apical margin of the tarsomere (Figure 3a). Its surface bears the same fine pubescence as the rest of the tarsus and its lateral proximal surface is covered with scales (Figures 1b and 3a). The thick and heavily sclerotized unguitractor plate is tapering distally (Figures 3c, 4c, and 5a). It is flanked by a pair of blade-like setae (ca. 0.2 mm long) with a low median longitudinal ridge. The unguitractor tendon inserts mesally on the proximal margin of the plate (Figure 4c), which bears a hook-shaped swelling distally on its dorsal surface (Figures 4c and 5c). A distinct pad-like planta (pl, Figures 1b, 3a, 4, and 5b,c) is connected with the dorsal hook by a membrane, with the distal edge of the unguitractor plate overlapping with the connecting area (Figures 4c and 5c). The planta is slightly narrower at the base than at its distal margin. It is slightly concave distally and the lateral edges more strongly rounded. It bears a dense vestiture of short, slightly curved setae. A pair of small auxilliary sclerites is visible laterodistad the unguitractor plate (Figures 3a and 4a,d,f). The well-developed, curved claws (cl, Figures 1a–c, 3a, and 4) bear a distinct slender tooth with a rounded apex approximately at mid-length. A short seta is inserted proximad this projection and a row of extremely short spines distad of it. The proximal part except for the ventral side bears the regular fine pubescence. A seta of about 0.1. mm length is inserted proximally on the glabrous distal half of the claws.

The pretarsal attachment apparatus is well developed and complex. The arolium (ar, Figures 1a–d, 3a, and 5a–c) is dorsally adjacent with the manubrium and resilin enriched. It is formed by two lobes separated by a deep median cleft. They are slightly broader than the manubrium at their base and distinctly widening toward the slightly convex apical margin. The surface of the highly flexible cuticle bears a very dense pattern of transverse folds resembling a fingerprint pattern (Figure 1d). The paired structures are rolled laterally in the resting position (Figure 1c). The surface structure of the apical margin displays a pattern of extremely small papillae, most of them with a minute cuticular thorn. The unsclerotized cuticle below this region of
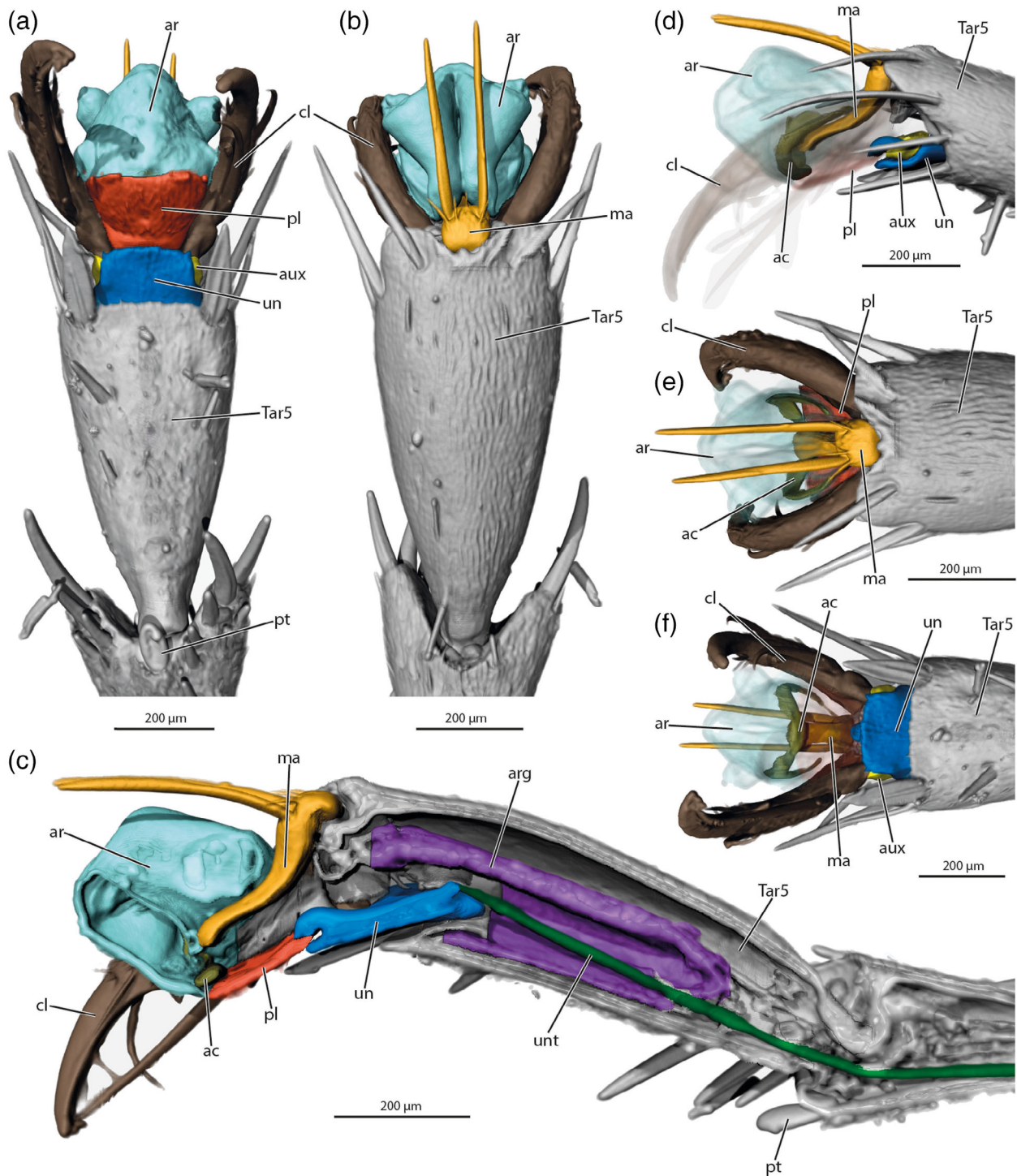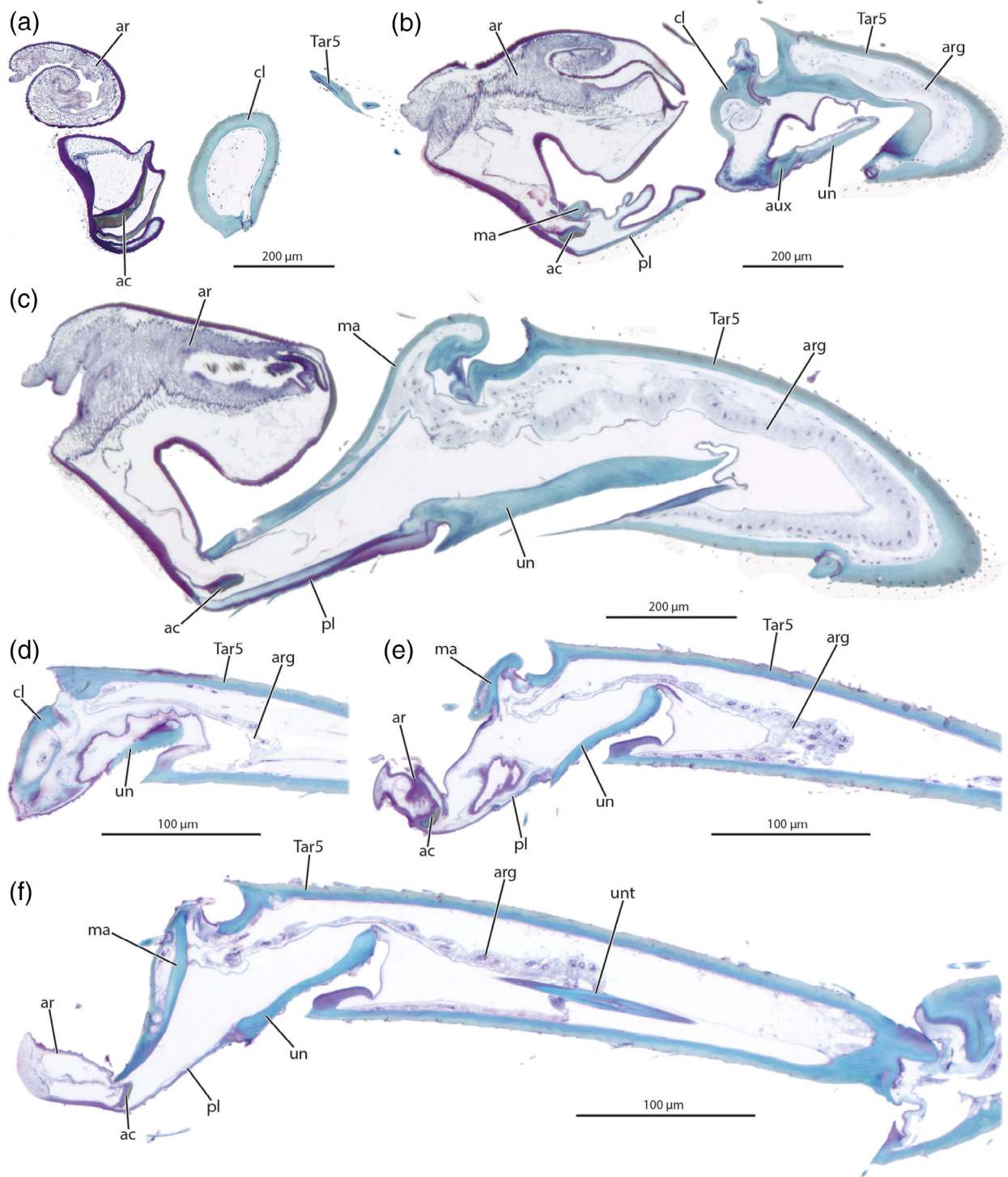
FIGURE 4 *S. caementarium* (Sphecidae), volume render images of tarsomere 5 of a female foreleg, (a) Protarsomere 5 ventral view. (b) Protarsomere 5 dorsal view. (c) Protarsomere 5 view of a sagittal section. (d) Lateral view of pretarsal structures with transparent arolium, claws, and planta. (e) Dorsal view of pretarsal structures with transparent arolium. (f) Ventral view of pretarsal structures with transparent arolium and planta. ar, arolium (turquoise); ac, arcus (green-brown); aux, auxiliary sclerites (yellow); arg, arolium gland (purple); cl, claw (brown); ma, manubrium (dark yellow); pl, planta (red); pt, plantula (gray); Tar5, tarsomere 5 (gray); un, unguitractor plate (blue); unt, unguitractor tendon (green)

the arolium is smooth and subdivided by several folds (Figure 1c). A large cushion-like membranous part of the arolium between this smooth area and the distal edge of the planta bears a dense vestiture of short, curved microtrichia (ca. 7 μm; Figure 1b,c). The clasp-shaped

arcus is a sclerotized internal flat band (ac, Figures 3a–c and 4d–f). It is located along the distal margin of the planta, running dorsad along the lateral sides of the ventral half of the arolium, not quite reaching its dorsal margin (Figure 4d).

FIGURE 5 *S. caementarium* (Sphecidae) (a–c) and *F. rufa* (Formicidae) (d–f), histological section microphotographies of tarsomere 5 of a female (worker in case of *Formica*) foreleg, *Sceliphron* sections are slightly longitudinally diagonal, *Formica* sections are longitudinal. (a–c) From lateral at the level of the basal claw to sagittal. (d–f) From lateral at the very base of the claw to sagittal. ar, arolium; ac, arcus; aux, auxiliary sclerites; arg, arolium gland; cl, claw; ma, manubrium; pl, planta; Tar5, tarsomere 5; un, unguitractor plate; unt, unguitractor tendon

3.3 | *F. rufa* (Formicidae, Formicinae)

The three slender legs differ in details of their armature and length. The length ratio of the tarsi from anterior to posterior is 2.5:3:4. The

forelegs differ by the distinct enlargement of the coxa and the presence of a well-developed antenna cleaner (Figures 1h and 2c,d). The middle and hind legs are similar in their general structure and setation pattern, even though the latter are distinctly longer. The coloration is

brownish and uniform. Almost the entire surface of the legs is covered with a pubescence of fine setae of about 0.025 mm length. Setae and spine-like setae of different length and shape are concentrated on the apical parts of the tarsomeres, and also inserted along the anterior and posterior edges and on the ventral side, but largely missing on the dorsal surface.

With a length of about 1.1 mm, the probasitarsomere is more than 1.5 times as long as the remaining segments combined. The basal part following the articulation with the tibia is distinctly curved. The basitarsal comb (btc, Figures 1h, 2c,d, and 3d), a slightly oblique, straight and dense row of stiff microtrichia (ca. 0.02 mm), is located in a shallow ventral concavity (ca. 0.4 mm long) on the proximal third of the segment. A narrow glabrous field is present between the comb and the posterior edge of the tarsomere (Figures 2d and 3d). The posterior edge bears a subregular row of strong setae (0.1–0.12 mm), whereas only few thinner setae are inserted on the anterior side. The anteroventral side of the tarsomere is densely covered with tenent hairs (Basibuyuk & Quicke, 1995: paddle-shaped setae) of about 0.1 mm length, each of them with a slightly extended spatulate apical part (Figures 1h and 2c). Several strong setae are present at the anterior and posterior apex (ca. 0.15 mm), the former less stout than the latter. An additional pair of setae is inserted subapically on the dorsal side. The apex of the tarsomere is truncated. A tarsal plantula is lacking like on the following tarsomeres.

The calcar (ca, Figures 2c,d and 3d) is inserted in an apical tibial notch like in *Sceliphron*, but with a much smaller and homogenously tough membranous pad (Figure 3d). The posterior spur is absent. The calcar is 0.56 mm long, straight in ventral view but sinuate viewed from lateral, and has a single pointed apex. It bears a straight, dense comb of tough and flexible microtrichia of about 0.03 mm length, adjacent to a narrow area of smooth cuticle, but without a transparent lamellum. The entire surface of the calcar bears a regular pubescence of short and fine microtrichia. A ventral row of teeth is missing.

Protarsomere 2 is about one-fourth as long as segment 1 (ca. 0.27 mm). The basal part articulated with the apex of the probasitarsomere is shaped like a narrow peduncle. The segment is moderately widening toward the apex, which is slightly emarginated on the dorsal side. The fine vestiture of the dorsal and ventral surface is similar to that of the dorsal side of tarsomere 1. Several pairs of spine-like setae insert between the fine setae on the ventral surface. The apical armature of spine-like setae is similar to that of tarsomere 1.

Protarsomere 3 is about 0.16 mm long. It is also articulated with a short peduncle and distinctly widening toward the apex. The vestiture and pattern of stronger setae is similar to that of the preceding segment. The apex is distinctly emarginated. Two pairs of strong and slightly flattened spine-like setae with an indistinct pattern of longitudinal riffles insert at the slightly extended anterior and posterior apices of the tarsomere, and an additional pair between them on the ventral side. Additionally, two groups of spine-like setae are present on the ventral surface, four closer to the anterior edge and three closer to the posterior margin.

Protarsomere 4 is again shorter (ca. 0.1 mm) than 3 and widening strongly toward the distinctly extended anterior and posterior apical

edges, which are separated by a distinct emargination. The basal peduncle is similar to that of tarsomeres 2 and 3. The vestiture of fine and spine-like setae is similar to the pattern on the preceding segment.

Protarsomere 5 is about twice as long as Segment 4, and similar in shape to tarsomere 2. The fine vestiture is similar to that of the preceding segments. The stronger setae at the apex and ventral surface are longer and thinner than those of the preceding tarsomeres. The dorsal apical margin displays rounded apical lobes separated by a median emargination (Figure 1g). A pair of long setae inserts close to the distal edge. The small rounded proximal end of the manubrium with a glabrous dorsal surface inserts in the emargination (Figure 1g). A pair of long setae (ca. 0.1 mm) inserts on the distal surface of the proximal manubrium (Figure 1g). The manubrium reaches deeply into the arolium (ma, Figures 1g, 5f, and 6c,d).

The well-sclerotized unguitractor plate (un, Figures 1e,h, 3b, 5d–f, and 6c) is rectangular with rounded corners, with most of the surface covered by a scaly pattern (Figure 3b). Relatively short and thin setae are distributed over the surface of the sclerite, mostly on the smooth distal part. A transverse line on the ventral side of tarsomere 5, shortly proximad the unguitractor plate (visible on CLSM images, Figure 3b), represents the inward-inflected distal margin of tarsomere 5 (Figure 5f). The planta is distally adjacent with the unguitractor plate (pl, Figures 1e,f,h, 3b, 5e,f, and 6a,c). A pair of setae of ca. 0.08 mm is inserted laterally on the base. Additional shorter setae are distributed over the surface of the sclerite. Auxiliary sclerites are not recognizable. The well-developed claws (cl, Figures 1e–h, 3b, and 5d) bear a dense pattern of short microtrichia on their basal part and an array of setae of different thickness and length, the strongest one inserted on the mesal edge directly distad the field of microtrichia. A tooth is not present. A distinct groove is present mesally on the distal half (Figure 1f).

The apically bilobed resilin-containing arolium (ar, Figures 1e–h, 3b, 5e, and 6a–c) is distinctly developed, but appears small compared to the claws. It is about 0.07 mm long and 0.05 mm wide near its base. On the dorsal surface and at the apical margin it bears a dense pattern of papillae with pointed spines (Figure 1g). The surface on the ventral side is smooth (Figure 1e). The arcus is not recognizable externally, but it is visible on microtome section series and μ-CT data as a thin, sclerotized structure similar to that of *Sceliphron* but shorter and not bent toward tarsomere 5 (ac, Figures 5e,f and 6c–e).

4 | CHARACTERS

1 Fine pubescence of legs: (0) present; (1) absent. A dense pubescence of short setae is present in Sphecidae and Formicidae, and also in other groups of Hymenoptera (e.g., Schulmeister, 2003, figure 1b,c). It is less regular and dense in Xyelidae (Schulmeister, 2003, figure 1a; Basibuyuk & Quicke, 1995). It is conceivable that this is a plesiomorphic feature preserved in this family. However, the character state polarity assessment is difficult in this case. The condition varies strongly in possible
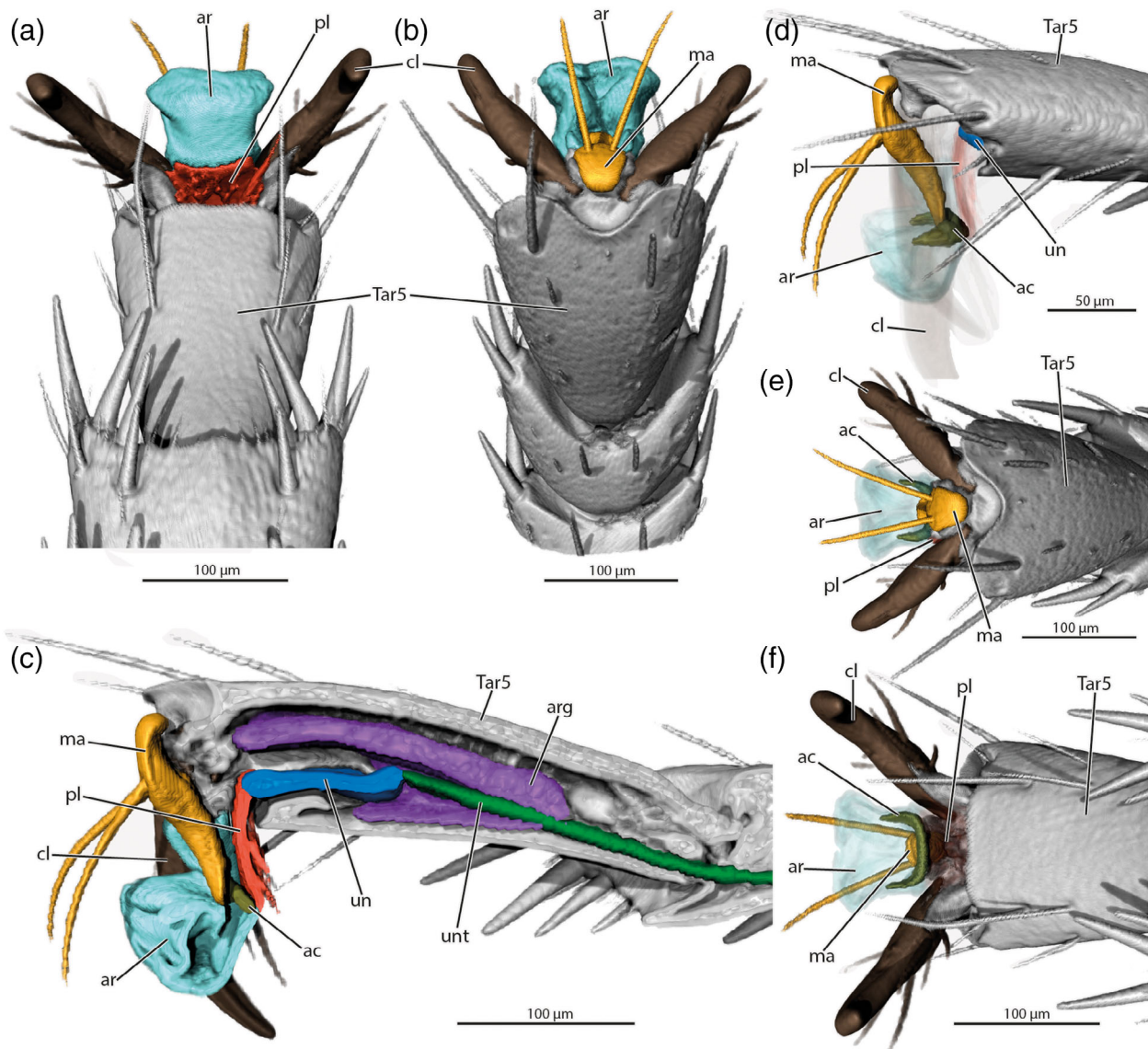
FIGURE 6 *F. rufa* (Formicidae), volume render images of tarsomere 5 of a female foreleg, (a) Protarsomere 5 diagonal ventral view. (a) Protarsomere 5 diagonal dorsal view. (c) Protarsomere 5 view of a sagittal section. (d) Lateral view of pretarsal structures with transparent arolium, claws, and planta. (e) Diagonal dorsal view of pretarsal structures with transparent arolium. (f) Diagonal ventral view of pretarsal structures with transparent arolium and planta. ar, arolium (turquoise); ac, arcus (green-brown); arg, arolium gland (purple); cl, claw (brown); ma, manubrium (dark yellow); pl, planta (red); Tar5, tarsomere 5 (gray); un, unguitractor plate (blue); unt, unguitractor tendon (green)

outgroups, such as for instance in Paraneoptera (Friedemann, Spangenberg, Yoshizawa, & Beutel, 2014, figures 1 and 3–5).

2 Distal tibial notch: (0) absent; (1) present. The anterior spur (calcar) is inserted in a distinct notch of the distal tibia in all hymenopteran species examined (see also Basibuyuk & Quicke, 1995, figures 1–4). This is likely a ground plan apomorphy of Hymenoptera.

3 Posterior protibial spur: (0) present; (1) absent (Basibuyuk & Quicke, 1995). Present in almost all symphytan groups and in the ground plan of Hymenoptera. Absent in Siricidae and Anaxyelidae, and almost generally missing in Apocrita including Sphecidae and Formicidae. Present in Megaspilidae and Ceraphronidae, and polymorphic in few families (Basibuyuk & Quicke, 1995).

4 Shape of anterior spur: (0) straight; (1) sinuate. The calcar is sinuate in *Sceliphron* and the ants examined, and also in most other groups of Hymenoptera. A curved anterior protibial spur is a ground plan apomorphy of Hymenoptera according to Basibuyuk and Quicke (1995) (see also Vilhelmsen (2001)).

5 Apex of anterior spur: (0) simple; (1) bifurcated. A bifurcated apex of the calcar occurs in Xyelidae and several other symphytan groups such as Pamphilidae, Tenthredinidae, and Orussidae, and also in apocritan groups like Evaniidae, Aulaciidae, Stephanidae, and others (Basibuyuk & Quicke, 1995, figures 1–4). Consequently, this is probably a ground plan apomorphy of Hymenoptera. The apex is simple in the groups we examined.

6 Inner comb of calcar: (0) absent; (1) present. The inner comb of the calcar is present in all the species examined. This is likely an autapomorphy of Hymenoptera.

7 Transparent lamellum of calcar (velum): (0) present; (1) absent. The velum is present in Xyelidae and other basal hymenopteran lineages (Basibuyuk & Quicke, 1995), and also in *Sceliphron* and in other apocritan groups. The lamellum is probably part of the ground plan of Hymenoptera, and probably also of Formicidae. However, it has been reduced many times independently in ants, and it is also absent in *Formica* (Basibuyuk & Quicke, 1995; Keller, 2011).

8 External row of tooth-like setae on calcar: (0) absent; (1) present. Present in *Sceliphron*. This is apparently a derived condition, but the origin within Apoidea is uncertain. The row is absent in basal groups of Hymenoptera (Basibuyuk & Quicke, 1995) and in the ants examined.

9 Sole of tenent setae on probasitarsomere: (0) absent; (1) present. A dense sole of tenent setae with a widened spatulate part (Basibuyuk & Quicke, 1995: paddle-shaped setae) is present in *Sceliphron*, in the ant species examined, and also in most other groups of Hymenoptera. Only a short row of few large paddle-shaped structures is present in *Macroxyela* (Basibuyuk & Quicke, 1995, figure 1a), arguably a plesiomorphic condition preserved in Xyelidae. The field of more or less densely arranged tenent setae reaches the apex of the protarsomere in Pamphilidae and other basal lineages of Hymenoptera (Basibuyuk & Quicke, 1995).

10 Tarsal plantulae: (0) present; (1) absent. Tarsal plantulae are present in the ground plan of Hymenoptera (Rasnitsyn, 1988). They are absent in most groups of Apocrita including extant Formicidae, but well-developed in *Sceliphron*.

11 Connection of plantulae with ventral tarsal surface: (0) integrated into ventral surface of tarsomeres; (1) distally articulated with tarsomeres. The tarsal plantulae are firmly integrated in the ventral sclerotized surface of tarsomeres 1–4 in Xyelidae and Pamphilidae (Schulmeister, 2003). They are articulated at the distal edge of the tarsomeres 1–4 in *Sceliphron*, and also in other groups of Hymenoptera (Schulmeister, 2003).

12 Number of tarsal plantulae on tarsomeres: (0) single plantula; (1) double plantula. Integrated double plantulae occur in Pamphilidae and articulated double plantulae in Xiphydriidae (Schulmeister, 2003). The presence of double plantulae is apparently a derived condition that evolved independently in the groups concerned.

13 Lateral lobate projections of protarsomeres 2–4: (0) absent or very indistinct; (1) distinct. Distinct lateral lobate projections are present on protarsomeres of *Formica* and *Cataglyphis*, especially on tarsomere 4, and also in *Vespula* (Frantsevich & Gorb, 2004). They are absent in Xyelidae and other basal lineages (e.g., Schulmeister, 2003, figure 1), and indistinct in *Sceliphron* and *Myrmecia* (Liu, Richter, Stoessel, & Beutel, 2019, figure 5a). Apparently, this condition varies strongly in Hymenoptera and also in Formicidae (Keller, 2011).

14 Strengthened ventral spine-like setae on distal region of protarsomeres 2–4: (0) absent; (1) present. An array of slightly curved spine-like setae is present on the distal part of the ventral side of protarsomeres 2–4 of *Formica*, especially on the lobate projections (see also Keller, 2011, figures 26a and 27c,d; Troya, 2012, figure 7b). Long and slender spine-like setae are present in *Cataglyphis*, whereas they are short and straight in *Myrmecia* (Liu et al., 2019, figure 5a). Curved and strengthened setae are missing in basal lineages of Hymenoptera (Schulmeister, 2003, figure 1). Blade-like setae are distally inserted on all tarsomeres in *Sceliphron*, and groups of short curved spine-like setae in *Vespula* (Frantsevich & Gorb, 2004, figure 4). More data are required for a phylogenetic assessment of this character, which is apparently variable in Hymenoptera and Formicidae (Keller, 2011).

15 Tooth of claw: (0) present; (1) absent. A tooth is present in *Sceliphron* and members of other hymenopteran lineages, but absent in *Formica* and *Cataglyphis* and other ant species examined. It was noted in Keller (2011) that the claws can vary strongly throughout the ant tree of life, for instance with a strongly developed tooth like in *Harpegnathos saltator* (T.C. Jerdon), with a pectinate mesal edge like in *Leptogenys* Roger sp., or with spiniform basal projections like in *Bothroponera pachyderma* Emery. Toothed claws also occur in fossil ant species (e.g., Barden, 2017).

16 Proximal pubescence of claws: (0) present; (1) absent. A proximal pubescent part of the claws was present in all species of Hymenoptera included in our sampling. It is missing in species of Chalicidoidea examined by Gladun & Gumovsky (2006: figs 7-9).

17 Manubrium: (0) absent; (1) present. The manubrium is generally present in Hymenoptera (e.g., Gladun, 2008; Snodgrass, 1956) and likely a ground plan apomorphy of the order. It is usually elliptical or quadrangular with rounded edges, but protruding distad in the ant *Xymmer muticus* (=*Amblyopone mutica* [Santschi]) (Keller, 2011).

18 Planta: (0) absent; (1) present. A planta is present in all species examined. An arrangement with the unguitractor followed by this plate-like structure supporting the arolium on the ventral side is likely a synapomorphy of Hymenoptera (e.g., Gladun, 2008).

19 Auxiliary sclerites (auxillae): (0) absent; (1) present. Auxiliary sclerites (Gladun, 2008) are almost generally present in the symphytan families but missing in Orussidae (Gladun, 2008). The presence is likely a ground plan apomorphy of Hymenoptera. The auxiliary sclerites are also commonly found in Apocrita (e.g., Gladun & Gumovsky, 2006, figure 1b), but are missing in Chalcidoidea and vestigial or absent in Formicidae.

20 Arolium: (0) present; (1) absent or vestigial. An arolium is generally present in Hymenoptera and likely a plesiomorphic ground plan feature of the order. Among Holometabola it is present in Neuroptera, Trichoptera (partim), Lepidoptera (most groups) and Mecoptera (excl. Boreidae and Nothiothaumidae; Beutel & Gorb, 2001). The arolium is well-developed in stem group ants (e.g., Barden & Grimaldi, 2012) and certainly belongs to the ground plan of the family. However, it is vestigial or absent in many

species in various groups, and the presence or absence of the arolium on the forelegs is not necessarily linked to its presence on the middle and hind legs (Keller, 2011).

21 Size of arolium: (0) about half as long as claws; (1) distinctly less than half as long as claws. The arolium of most hymenopteran groups is at least half as long as the claws or almost as long (e.g., Frantsevich & Gorb, 2002; Gladun, 2008, figures 1–3). It is distinctly reduced in size even in ant groups where it is distinctly developed.

22 Arcus: (0) absent; (1) present. The arcus is present in the species examined. It is usually difficult to identify in ants with preserved arolia (see char. 20), but distinctly developed in *Formica* (Figure 6c,d,f). The structure is very likely a ground plan apomorphy of Hymenoptera. It is reduced in females of Siricidae (Gladun, 2008) and very likely missing in the ants with vestigial arolia. It is unclear at present whether the unfolding mechanism described by Snodgrass (1956) and Frantsevich and Gorb (2002) is retained in the ground plan of Formicidae. A laterally folded (or rolled) resting condition (e.g., *Sceliphron*) was not observed in any ant species of our sampling.

5 | DISCUSSION

5.1 | Phylogenetic interpretations

Hymenoptera differ from all other groups of hemimetabolous or holometabolous insects (see Beutel & Gorb, 2001, 2006; Gorb & Beutel, 2001) by a triple set of tarsal and pretarsal attachment structures: tarsal plantulae (Schulmeister, 2003), spatulate (or paddle-shaped) setae on the ventral side of the probasitarsomere (Basibuyuk & Quicke, 1995), and a well-developed arolium with an arcus inside and a pretarsal planta (e.g., Gladun, 2008). This combination is part of the hymenopteran ground plan, and a complex evolutionary innovation and autapomorphy of the order. The probasitarsal adhesive sole and a complex arolium are almost generally preserved in the order, whereas the plantulae are missing in different groups, especially in Apocrita. The plantulae are very likely fixed in the ground plan of Hymenoptera, as it is the case in Xyelidae and Pamphilidae, but usually articulated and shifted to the distal edge of the tarsomeres in groups where they are present. The manubrium and planta, plate-like dorsal and ventral structures enclosing the arolium, are also ground plan apomorphies of the order, and probably also the small lateral auxiliae. The former are generally present, whereas the latter are vestigial or missing in different groups, for instance in Formicidae. A unique apomorphy of Hymenoptera is the arcus, a spring-like structure functioning as an extending mechanism of the arolium, thus increasing its efficiency as an attachment structure (Frantsevich & Gorb 2002).

The presence of paddle-shaped (or spatulate) tenent setae on the probasitarsomere is likely an autapomorphy of the order. Hairy adhesive soles also occur in the orders of Neuropterida (in Megaloptera and Raphidioptera) and Coleopterida (in Stylopidia [Strepsiptera] and

many groups of Coleoptera; e.g., Beutel & Gorb, 2001; Pohl & Beutel, 2004). However, they are likely not part of the ground plan of both large lineages and are not restricted to the probasitarsomere as it is the case in Hymenoptera.

A curved or sinuate tibial calcar, in most groups interacting with the strigil of the probasitarsomere as cleaning device, is a derived feature preserved throughout Hymenoptera. A transparent velum is likely present in the ground plan, but occasionally reduced, for instance in *Formica* and various other Formicidae. The calcar is likely bifurcated at the apex in the ground plan, but only a single apex is present in most groups, probably a transformation that took place several times among symphytan groups and in Apocrita. The apical tibial notch, the insertion site of the calcar, is probably an additional apomorphy of Hymenoptera, whereas the ventral concavity or notch of the probasitarsomere containing the strigil is likely a synapomorphy of Orussidae and Apocrita (Vilhelmsen et al., 2010).

Xyelidae differ distinctly in their leg structures from other groups of Hymenoptera. Whereas the surface of all three pairs of legs usually bears a very dense vestiture of fine setae, this pattern is less dense in this family, where glabrous areas of the cuticle display a reticulate microstructure (Basibuyuk & Quicke, 1995, figure 1). This is arguably a ground plan condition of Hymenoptera, even though secondary modification of the fine setation in Xyelidae cannot be excluded. Another presumptive plesiomorphy found in Xyelidae, and also in Pamphilidae, is the lacking articulation of the plantulae and their proximal position. A feature of Xyelidae different form all other groups is the short single row of relatively large paddle-shaped setae on the probasitarsomere. The polarity of this character is ambivalent like in the case of the fine setation of the legs. The condition found in Xyelidae could be a preserved plesiomorphy or an autapomorphy of the family. In the former case, a dense pattern of tenent setae would be a potential apomorphy of Hymenoptera excl. Xyelidae (e.g., Beutel & Vilhelmsen, 2007; Vilhelmsen, 1997). The alternative, secondary simplification conforms with a placement of Xyelidae as second branch (after Pamphiloidea) in monophyletic Eusymphyta, as suggested in a recent transcriptomic study (Peters et al., 2017; but see Branstetter, Danforth, et al., 2017). In addition to a secondarily shortened simple row of paddle-shaped tenent hairs in Xyelidae, this phylogenetic concept implies the secondary loss of the ability of males of this family to restore diploidy in their muscles (Peters et al., 2017), independent gain of articulated tarsal plantulae in groups assigned to Eusymphyta, and also independent losses of mandibular molae and epipharyngeal brushes (Beutel & Vilhelmsen, 2007). Moreover, it implies homoplasy in the case of several features suggested by Vilhelmsen (2001) for Hymenoptera excl. Xyelidae: well-developed cervical apodemes, mesothoracic postspiracular sclerites, the absence of the metapleural-S2 muscles, the presence of only one branch in Rs, and possibly the adecticous pupae (Hinton, 1971).

Formicidae have retained most of the typical hymenopteran equipment of the legs, and considering the ground plan of the family differ scarcely from related groups. It appears likely that the distal elements of ants are primarily adapted to the ground-oriented lifestyle (Lucky, Trautwein, Guenard, Weiser, & Dunn, 2013; Nelsen, Ree, &

Moreau, 2018) of most ants, and an increased necessity to clean the body surface due to their eusocial nature that requires intensive interaction among individuals. However, it has to be noted that reproductive males and females fly and land on various surfaces in a "wasp-like" manner. This could explain why ant legs are not strongly modified compared to the hymenopteran ground plan.

A vague characteristic at best is the tendency to elongate the legs in relation to the body size. This character varies enormously within Formicidae, and also in other hymenopteran groups. Moreover, short legs are characteristic for soil dwelling ants and species adapted to burrow in sticks or branches, and elongated legs occur in different apocritan groups, for instance in the chrysidoid Dryinidae or the vespoid Pompilidae (Grimaldi & Engel, 2005). As cleaning the body surface and especially sensilla on the antennae and other parts is apparently important for these eusocial insects, the cleaning apparatus of the protibia and probasitarsus is fully developed, except for some minor modifications like the absence of the velum, which is variably lost at the subfamily level, in addition to the genus level. A dense brush on the calcar and in the probasitarsomeral notch are probably generally present in Formicidae, and slightly less complex cleaning devices also occur on the middle and hind legs (Liu et al., 2019: _Myrmecia_).

In contrast to the cleaning apparatus, the complex of adhesive structures of ants shows some distinct modifications, tentatively suggesting ground oriented habits in the ground plan of Formicidae. The sole of tenent setae of the probasitarsomere is likely generally present. In contrast to this, plantulae are always absent in extant ants, a feature also found in most other groups of Aculeata, but not in Sphecidae. The arolium is present in the ground plan of crown group Formicidae, but appears distinctly smaller than in related groups, like for instance Sphecidae or Vespidae (Frantsevich & Gorb, 2002). It is vestigial in _Ectatomma tuberculatum_ and _Odontomachus hastatus_ (Keller, 2011; Troya, 2012), but distinct even though small in relation to the claws in other groups, and distinct in extinct groups (e.g., Barden & Grimaldi, 2012). The manubrium and planta are well-developed in the ant species examined.

A detailed assessment of the distal leg structures across the ant phylogeny to reconstruct the evolution of this character system within Formicidae is currently not available. Whether the unfolding mechanism of the arolium described in detail for species of Vespidae by Frantsevich and Gorb (2002) is present in the ground plan of Formicidae is still unclear. The presence of curved spine-like setae on the distal part of the ventral sides of the tarsomeres, especially on the lobate projections, likely plays a role in improved locomotion on irregular surfaces, such as soil or strongly sculptured plant surfaces (Frantsevich and Gorb, 2002, 2004). This character varies strongly within Formicidae, even including different pairs of legs (Keller, 2011).

5.2 | Functional aspects

In this section, we focus on two different functional aspects of the distal hymenopteran leg: (a) antennal cleaning organ and (b) attachment structures. Our CLSM study provides some insights

about material compositions in these structural elements, which might give us further information on local physical properties of the cuticle material.

Such information has been obtained for the antennal cleaning organ for the first time. Different autofluorescence levels suggest different material composition and properties of the basitarsal comb and calcar of the strigil. Additionally, both structures reveal gradients of physical properties in both analyzed species. Likewise, in both species, either the basitarsal comb or the calcar of the strigil is distinctly more flexible than the counterpart. This is arguably an adaptation for efficient removal of particles of different sizes and adhesive properties from the antennae. Insects must be able to remove dust particles or detritus firmly glued to the cuticle, but at the same time avoid damaging the delicate antennal sensory equipment and minute microstructures of the cleaning device. Therefore, the observed differences in material composition and physical properties might be an optimized solution for these two interrelated problems. However, it remains unclear, why the basitarsal comb is more flexible than the calcar in _Formica_, while it is the other way around in _Sceliphron_, as revealed by our CLSM based observations. This approach and results open a wide field for further functional morphological study on the antennal cleaner in Hymenoptera.

As in many other groups of insects, the hymenopteran distal leg combines two functional mechanisms adapted to reliable attachment to substrates with unpredictable properties: (a) an interlocking-based one (claws and spine-like setae) and (b) an adhesion-based one (arolium and plantae). On rough substrate, claws interlock with surface asperities and secure a firm grip, whereas on smooth substrate, the claws slip off the surface, while the arolium unfolds and generates adhesive contact (Federle, Brainerd, McMahon, & Hölldobler, 2001; Frantsevich & Gorb, 2002, 2004; Snodgrass, 1956). However, on an intermediate range of substrate roughness, depending on the specific degree of surface irregularity, both these mechanisms can either work in concert or completely fail (Frantsevich & Gorb, 2004). The combined action of both mechanisms was recently tested in an experiment evaluating a rather simple mechanical model (Song, Dai, Ji, & Gorb, 2016).

The tarsal chain is an important part of the attachment mechanism, especially for alignment on different substrate curvatures (Gladun & Gorb, 2007). The articulations in the tibial-tarsal-pretarsal kinematic chain are multiaxial (Frantsevich & Gorb, 2004; Snodgrass, 1956), but with the contraction of the claw retractor muscle, the arolium turns forward and downward simultaneously accompanied by a flexion of the claws. It has been previously shown and is supported by the present study that articulations between tarsomeres and different elements within the pretarsus are surrounded with elastic cuticle containing resilin. The elastic elements ensure a prompt extension of the tarsus after relaxation of the retractor muscle and the removal of the load from the arolium and/or claws (Snodgrass, 1956).

Previous data on walking techniques of sphecid wasps (_Mellinus arvensis_ [Linnaeus]) and formicine ants (_Formica polyctena_ Förster) showed that they use contact of distal tarsomeres of overextended

tarsi on flat surfaces (Gladun & Gorb, 2007), whereas they have difficulties to walk on a thin horizontal rod. In the latter situation, fore and hind legs rely either on distal tarsomeres or on the center of the overextended or slightly bent tarsus. If the middle part of the tarsus is used in contact, distal tarsomeres (especially of the midlegs) do not touch the substrate. Climbing upward on rods requires labor division between different pairs of legs (Gladun & Gorb, 2007). While walking up a thin rod, the fore tarsi of *F. polyctena* ants often clutch the substrate with the claws. Ants can walk down thin vertical rods, but sphecid wasps were not able to do this (Gladun & Gorb, 2007). These differences might be related to the differences in the relative dimensions between the tarsi and substrate curvature in sphecid wasps and ants. Additionally, relatively longer tarsi of ants may support running down thin rod-like objects. Walking on distal tarsomeres, observed in wasps and ants, is presumably an apomorphic character of Hymenoptera (Frantsevich & Gorb, 2004), in contrast to walking on the entire tarsus in some other insects, such as for instance beetles.

The presumed specialization of ants for efficient locomotion on the ground is also documented by their remarkable ability to stay on surfaces or regain contact with a surface in microgravity on the International space station (Countryman et al., 2015).

The hairy coverage at the bottom of the distal tarsomeres presumably plays a role in preventing slipping during walking on horizontal surfaces, when other attachment structures such as the claws or arolium are not necessarily in contact with the substrate. Elastic ends of the hairs (with a higher resilin concentration) may enter microcrevices of the substrate and provide thousands of interlocking sites contributing to the overall friction (Frantsevich & Gorb, 2004). The tarsal plantulae of *Sceliphron*, due to their soft properties, might additionally increase friction on horizontal flat substrates, and enhance grasping efficiency of the wasp during transportation of items in flight. These structures are also widespread in symphytan groups, where they might provide strong anchorage on the substrate during oviposition into plant tissue. *Oecophylla smaragdina* Fabricius (Formicinae) climbing efficiently on smooth vertical surfaces was investigated by Endlein and Federle (2015). The authors could demonstrate that the weaver ants do not only use their arolia, but also dense arrays of fine setae on the ventral side of tarsomeres 3 and 4.

The unfolding mechanism of the arolium is rather complex, because it lacks real solid or rigid condylar joints except the articulation between the base of the manubrium and two sockets in the dorsal edge of the fifth tarsomere (Baur & Gorb, 2001; Federle et al., 2001; Frantsevich & Gorb, 2004). The soft and compliant nature of the arolium pad is due to an internal meshwork of dendrite-like filaments filled with the fluid in between (Baur & Gorb, 2001; Federle et al., 2001). The observed differences between *Sceliphron* and *Formica* in the folded arolium configuration presumably correlate with the differences in the mechanism of folding/unfolding, which is size-dependent in different groups of Hymenoptera. It has been previously demonstrated that bees and hornets use mainly the sclerite-mechanics-based unfolding mechanism (Federle et al., 2001; Frantsevich & Gorb, 2004), whereas ants use the hydraulically driven one (Federle et al., 2001).

Depending on the specific biology of the specific ant (or wasp) species and their substrate preferences, tarsal and pretarsal structures may have evolved additional specializations, especially in the arolium dimensions and specific shapes of the claws (Billen, Al-Khalifa, & Silva, 2017).

The present work will be the foundation of a future project on the evolution of distal leg structures in Formicidae and other groups of Aculeata. Our results show that while most of the general anatomical structures are conserved in ants, there are some distinct modifications probably related to a ground dwelling and social lifestyle. Comparisons with the literature also reveal considerable variation within Formicidae, for instance with regard to different levels of reduction of the arolium. The present study will be the starting point of more extensive investigations comparing distal leg structures across the Formicidae and reconstructing the evolution of this character system across the entire family.

CONFLICT OF INTEREST

The authors declare no potential conflict of interest.

AUTHOR CONTRIBUTIONS

Rolf Georg Beutel, Stanislav N. Gorb, and Evan P. Economo have designed the project. The µCT-data were provided by Adrian Richter, Francisco Hita-Garcia and Evan P. Economo. Adrian Richter and Yoko Matsumura documented the structural features with CLSM and SEM, and Adrian Richter did the 3D reconstructions based on µCT data. Roberto A. Keller has contributed rich information on structural features of ants and the variation within the group. All authors have participated in writing the manuscript and all have commented on the

final version. Stanislav N. Gorb wrote the section on functional aspects.

DATA AVAILABILITY STATEMENT

ORCID

Adrian Richter https://orcid.org/0000-0001-5627-2302

REFERENCES

Barden, P. (2017). Fossil ants (Hymenoptera: Formicidae): Ancient diversity and the rise of modern lineages. *Myrmecological News*, *24*, 1–30.

Barden, P., & Grimaldi, D. (2012). Rediscovery of the bizarre cretaceous ant *Haidomyrmex* Dlussky (Hymenoptera: Formicidae), with two new species. *American Museum Novitates*, *2012*(3755), 1–16.

Basibuyuk, H. H., & Quicke, D. L. (1995). Morphology of the antenna cleaner in the Hymenoptera with particular reference to non-aculeate families (Insecta). *Zoologica Scripta*, *24*(2), 157–177.

Basibuyuk, H. H., & Quicke, D. L. (1999). Grooming behaviours in the Hymenoptera (Insecta): potential phylogenetic significance. *Zoological Journal of the Linnean Society*, *125*(3), 349–382.

Baur, F., & Gorb, S. N. (2001). How the bee releases its leg attachment devices. In A. Wisser & W. Nachtigall (Eds.), *Technische Biologie und Bionik. 5. Bionik−Kongress, Dessau 2000* (pp. 295–297). Stuttgart: Gustav Fischer Verlag.

Beutel, R. G. (1992). Phylogenetic analysis of thoracic structures of Carabidae (Coleoptera: Adephaga). *Journal of Zoological Systematics and Evolutionary Research*, *30*(1), 53–74.

Beutel, R. G., Friedrich, F., Yang, X.-K., & Ge, S.-Q. (2014) *Insect Morphology and Phylogeny: a Textbook for Students of Entomology*. Berlin, New York: Walter de Gruyter.

Beutel, R. G., & Gorb, S. N. (2001). Ultrastructure of attachment specializations of hexapods (Arthropoda): evolutionary patterns inferred from a revised ordinal phylogeny. *Journal of Zoological Systematics and Evolutionary Research*, *39*(4), 177–207.

Beutel, R. G., & Gorb, S. N. (2006). A revised interpretation of the evolution of attachment structures in Hexapoda with special emphasis on Mantophasmatodea. *Arthropod Systematics & Phylogeny*, *64*(1), 3–25.

Beutel, R. G., & Gorb, S. N. (2008). Evolutionary scenarios for unusual attachment devices of Phasmatodea and Mantophasmatodea (Insecta). *Systematic Entomology*, *33*(3), 501–510.

Beutel, R. G., & Vilhelmsen, L. (2007). Head anatomy of Xyelidae (Hexapoda: Hymenoptera) and phylogenetic implications. *Organisms Diversity & Evolution*, *7*(3), 207–230. http://dx.doi.org/10.1016/j.ode.2006.06.003

Billen, J., Al-Khalifa, M. S., & Silva, R. R. (2017). Pretarsus structure in relation to climbing ability in the ants *Brachyponera sennaarensis* and *Daceton armigerum*. *Saudi Journal of Biological Sciences*, *24*, 830–836.

Brainerd, E. L. (1994). Adhesion force of ants on smooth surfaces. *American Zoologist*, *34*, 128–128.

Branstetter, M. G., Danforth, B. N., Pitts, J. P., Faircloth, B. C., Ward, P. S., Buffington, M. L., ... Brady, S. G. (2017). Phylogenomic insights into the evolution of stinging wasps and the origins of ants and bees. *Current Biology*, *27*(7), 1019–1025.

Branstetter, M. G., Longino, J. T., Ward, P. S., & Faircloth, B. C. (2017). Enriching the ant tree of life: Enhanced UCE bait set for genome-scale phylogenetics of ants and other Hymenoptera. *Methods in Ecology and Evolution*, *8*(6), 768–776.

Bullock, J. M., Drechsler, P., & Federle, W. (2008). Comparison of smooth and hairy attachment pads in insects: Friction, adhesion and mechanisms for direction-dependence. *Journal of Experimental Biology*, *211*(20), 3333–3343.

Countryman, S. M., Stumpe, M. C., Crow, S. P., Adler, F. R., Greene, M. J., Vonshak, M., & Gordon, D. M. (2015). Collective search by ants in microgravity. *Frontiers in Ecology and Evolution*, *3*, 25.

Dashman, T. (1953). Terminology of the pretarsus. *Annals of the Entomological Society of America*, *46*(1), 56–62.

De Meijere, J. C. (1901). Über das letzte Glied der Beine bei den Arthropoden. *Zoologische Jahrbücher. Abteilung für Anatomie und Ontogenie der Tiere*, *14*, 417–476.

Drechsler, P., & Federle, W. (2006). Biomechanics of smooth adhesive pads in insects: Influence of tarsal secretion on attachment performance. *Journal of Comparative Physiology A*, *192*(11), 1213–1222.

Endlein, T., & Federle, W. (2015). On heels and toes: How ants climb with adhesive pads and tarsal friction hair arrays. *PLoS One*, *10*(11), e0141269.

Engelkes, K., Friedrich, F., Hammel, J. U., & Haas, A. (2018). A simple setup for episcopic microtomy and a digital image processing workflow to acquire high-quality volume data and 3D surface models of small vertebrates. *Zoomorphology*, *137*(1), 213–228.

Federle, W., Brainerd, E. L., McMahon, T. A., & Hölldobler, B. (2001). Biomechanics of the movable pretarsal adhesive organ in ants and bees. *Proceedings of the National Academy of Sciences of the United States of America*, *98*(11), 6215–6220.

Federle, W., Maschwitz, U., Fiala, B., Riederer, M., & Hölldobler, B. (1997). Slippery ant-plants and skilful climbers: Selection and protection of specific ant partners by epicuticular wax blooms in *Macaranga* (Euphorbiaceae). *Oecologia*, *112*, 217–224.

Federle, W., Rohrseitz, K., & Hölldobler, B. (2000). Attachment forces of ants measured with a centrifuge: Better "wax-runners" have a poorer attachment to a smooth surface. *Journal of Experimental Biology*, *203*, 505–512.

Francoeur, A., & Loiselle, R. (1988). Évolution du strigil chez les formicides. *Le Naturaliste Canadien*, *115*, 333–353.

Frantsevich, L., & Gorb, S. (2002). Arcus as a tensegrity structure in the arolium of wasps (Hymenoptera: Vespidae). *Zoology*, *105*(3), 225–237.

Frantsevich, L., & Gorb, S. (2004). Structure and mechanics of the tarsal chain in the hornet, *Vespa crabro* (Hymenoptera: Vespidae): Implications on the attachment mechanism. *Arthropod Structure & Development*, *33*(1), 77–89.

Friedemann, K., Spangenberg, R., Yoshizawa, K., & Beutel, R. G. (2014). Evolution of attachment structures in the highly diverse Acercaria (Hexapoda). *Cladistics*, *30*(2), 170–201.

Gladun, D., & Gorb, S. N. (2007). Insect walking techniques on thin stems. *Arthropod-Plant Interactions*, *1*, 77–91.

Gladun, D., Gorb, S. N., & Frantsevich, L. I. (2009). Alternative tasks of the insect arolium with special reference to Hymenoptera. In *Functional Surfaces in Biology* (pp. 67–103). Dordrecht: Springer.

Gladun, D., & Gumovsky, A. (2006). The pretarsus in Chalcidoidea (Hymenoptera Parasitica): Functional morphology and possible phylogenetic implications. *Zoologica Scripta*, *35*(6), 607–626.

Gladun, D. V. (2008). Morphology of the pretarsus of the sawflies and horntails (Hymenoptera: 'Symphyta'). *Arthropod Structure & Development*, *37*(1), 13–28.

Gorb, S., & Beutel, R. G. (2001). Evolution of locomotory attachment pads of hexapods. *Naturwissenschaften*, *88*, 530–534.

Gorb, S. N. (2010). Biological and biologically inspired attachment systems. In *Springer Handbook of Nanotechnology* (pp. 1525–1551). Berlin: Springer.

Grimaldi, D., & Engel, M. S. (2005). *Evolution of the Insects*. Cambridge: Cambridge University Press.

Hackmann, A., Delacave, H., Robinson, A., Labonte, D., & Federle, W. (2015). Functional morphology and efficiency of the antenna cleaner in *Camponotus rufifemur* ants. *Royal Society Open Science*, *2*(7), 150129.

Hinton, H. E. (1971). Some neglected phases in metamorphosis. *Proceedings of the Royal Entomological Society of London, Series C, 35*(11), 55–63.

Hölldobler, B., & Palmer, J. M. (1989). Footprint glands in *Amblyopone australis* (Formicidae, Ponerinae). *Psyche, 96*(1–2), 111–121.

Johnson, B. R., Borowiec, M. L., Chiu, J. C., Lee, E. K., Atallah, J., & Ward, P. S. (2013). Phylogenomics resolves evolutionary relationships among ants, bees, and wasps. *Current Biology, 23*(20), 2058–2062.

Keller, R. A. (2011). A phylogenetic analysis of ant morphology (Hymenoptera: Formicidae) with special reference to the poneromorph subfamilies. *Bulletin of the American Museum of Natural History, 355*, 1–90.

Kristensen, N. P., & Skalski, A. W. (1999). Phylogeny and palaeontology. In Handbook of Zoology, Vol. IV. *Lepidoptera, Moths and Butterflies. Volume 1: Evolution, Systematics and Biogeography* (pp. 7–25). Berlin & New York: Walter de Gruyter.

Lambkin, C. L., Sinclair, B. J., Pape, T., Courtney, G. W., Skevington, J. H., Meier, R., ... Wiegmann, B. M. (2013). The phylogenetic relationships among infraorders and superfamilies of Diptera based on morphological evidence. *Systematic Entomology, 38*(1), 164–179.

Liu, S. P., Richter, A., Stoessel, A., & Beutel, R. G. (2019). The mesosomal anatomy of *Myrmecia nigrocincta* workers and evolutionary transformations in Formicidae (Hymenoptera). *Arthropod Systematics and Phylogeny, 77*(1), 1–19.

Lucky, A., Trautwein, M. D., Guenard, B. S., Weiser, M. D., & Dunn, R. R. (2013). Tracing the rise of ants-out of the ground. *PLoS One, 8*, e84012.

McKenna, D. D., Shin, S., Ahrens, D., Balke, M., Beza-Beza, C., Clarke, D. J., ... Letsch, H. (2019). The evolution and genomic basis of beetle diversity. *Proceedings of the National Academy of Sciences, 116*(49), 24729–24737.

Michels, J., & Gorb, S. N. (2012). Detailed three-dimensional visualization of resilin in the exoskeleton of arthropods using confocal laser scanning microscopy. *Journal of Microscopy, 245*(1), 1–16.

Misof, B., Liu, S., Meusemann, K., Peters, R. S., Donath, A., Mayer, C.,... Beutel, R. G. (2014). Phylogenomics resolves the timing and pattern of insect evolution. *Science, 346*(6210), 763–767.

Naumann, I. (1991). Hymenoptera. *The Insects of Ausalia*. Vol. 2, 2nd edn. Carlton, Australia: Melbourne University Press.

Nelsen, M. P., Ree, R. H., & Moreau, C. S. (2018). Ant–plant interactions evolved through increasing interdependence. *Proceedings of the National Academy of Sciences of the United States of America, 115*(48), 12253–12258.

Orivel, J., Malherbe, M. C., & Dejean, A. (2001). Relationships between pretarsus morphology and arboreal life in ponerine ants of the genus *Pachycondyla* (Formicidae: Ponerinae). *Annals of the Entomological Society of America, 94*(3), 449–456.

Peters, R. S., Krogmann, L., Mayer, C., Donath, A., Gunkel, S., Meusemann, K., ... Niehuis, O. (2017). Evolutionary history of the Hymenoptera. *Current Biology, 27*(7), 1013–1018.

Pohl, H., & Beutel, R. G. (2004). Fine structure of adhesive devices of Strepsiptera (Insecta). *Arthropod Structure and Development, 33*, 31–43.

Pohl, H. (2010). A scanning electron microscopy specimen holder for viewing different angles of a single specimen. *Microscopy Research and Technique, 73*(12), 1073–1076.

Rasnitsyn, A. P. (1988). An outline of evolution of the hymenopterous insects. *Oriental Insects, 22*, 115–145.

Regier, J. C., Mitter, C., Zwick, A., Bazinet, A. L., Cummings, M. P., Kawahara, A. Y., ... Mitter, K. T. (2013). A large-scale, higher-level, molecular phylogenetic study of the insect order Lepidoptera (moths and butterflies). *PLoS One, 8*(3), e58568.

Ronquist, F., Klopfstein, S., Vilhelmsen, L., Schulmeister, S., Murray, D. L., & Rasnitsyn, A. P. (2012). A total-evidence approach to dating with fossils, applied to the early radiation of the Hymenoptera. *Systematic Biology, 61*(6), 973–999.

Ronquist, F., Rasnitsyn, A. P., Roy, A., Eriksson, K., & Lindgren, M. (1999). Phylogeny of the Hymenoptera: A cladistic reanalysis of Rasnitsyn's (1988) data. *Zoologica Scripta, 28*(1–2), 13–50.

Sann, M., Niehuis, O., Peters, R. S., Mayer, C., Kozlov, A., Podsiadlowski, L., ... Ohl, M. (2018). Phylogenomic analysis of Apoidea sheds new light on the sister group of bees. *BMC Evolutionary Biology, 18*(1), 71.

Schönitzer, K., Dott, H., & Melzer, R. R. (1996). The antenna cleaner gland in *Messor rufitarsis* (Hymenoptera, Formicidae). *Tissue and Cell, 28*(1), 107–113.

Schönitzer, K., & Lawitzky, G. (1987). A phylogenetic study of the antenna cleaner in Formicidae, Mutillidae, and Tiphiidae (Insecta, Hymenoptera). *Zoomorphology, 107*(5), 273–285.

Schulmeister, S. (2003). Morphology and evolution of the tarsal plantulae in Hymenoptera (Insecta), focussing on the basal lineages. *Zoologica Scripta, 32*(2), 153–172.

Sharkey, M. J., Carpenter, J. M., Vilhelmsen, L., Heraty, J., Liljeblad, J., Dowling, A. P. G., ... Wheeler, W. C. (2012). Phylogenetic relationships among superfamilies of Hymenoptera. *Cladistics, 28*(1), 80–112.

Snodgrass, R. E. (1956). *Anatomy of the honey bee*. New York, NY: Comstock Publishing Associates.

Song, Y., Dai, Z., Ji, A., & Gorb, S. N. (2016). The synergy between the insect-inspired claws and adhesive pads increases the attachment ability on various rough surfaces. *Scientific Reports, 6*(26219), 1–9.

Troya, A. (2012). *Speciation of ants in the tropics of South America*. (master's thesis). Ludwig Maximilians Universität, München.

Valentine, B. D. (1986). Grooming behavior in Embioptera and Zoraptera (Insecta). *The Ohio Journal of Science, 86*(4), 150–152.

Vilhelmsen, L. (2001). Phylogeny and classification of the extant basal lineages of the Hymenoptera (Insecta). *Zoological Journal of the Linnean Society, 131*(4), 393–442.

Vilhelmsen, L. (1997). The phylogeny of lower Hymenoptera (Insecta), with a summary of the early evolutionary history of the order. *Journal of Zoological Systematics and Evolutionary Research, 35*(2), 49–70.

Vilhelmsen, L., Miko, I., & Krogmann, L. (2010). Beyond the wasp-waist: Structural diversity and phylogenetic significance of the mesosoma in apocritan wasps (Insecta: Hymenoptera). *Zoological Journal of the Linnean Society, 159*(1), 22–194.